Demonstration of High-Trapping Efficiency and Narrow Energy Spread in a Laser-Driven Accelerator

W. D. Kimura,[1,*] M. Babzien,[2] I. Ben-Zvi,[2] L. P. Campbell,[1] D. B. Cline,[3] C. E. Dilley,[1] J. C. Gallardo,[2] S. C. Gottschalk,[1] K. P. Kusche,[2] R. H. Pantell,[4] I. V. Pogorelsky,[2] D. C. Quimby,[1] J. Skaritka,[2] L. C. Steinhauer,[5] V. Yakimenko,[2] and F. Zhou[3]

[1]*STI Optronics, Inc., Bellevue, Washington 98004, USA*
[2]*Brookhaven National Laboratory, Upton, New York 11973, USA*
[3]*University of California, Los Angeles, Los Angeles, California 90095, USA*
[4]*Stanford University, Stanford, California 94305, USA*
[5]*Redmond Plasma Physics Laboratory, University of Washington, Redmond, Washington 98052, USA*
(Received 25 August 2003; revised manuscript received 23 January 2004; published 6 February 2004)

Laser-driven electron accelerators (laser linacs) offer the potential for enabling much more economical and compact devices. However, the development of practical and efficient laser linacs requires accelerating a large ensemble of electrons together (''trapping'') while keeping their energy spread small. This has never been realized before for any laser acceleration system. We present here the first demonstration of high-trapping efficiency and narrow energy spread via laser acceleration. Trapping efficiencies of up to 80% and energy spreads down to 0.36% (1σ) were demonstrated.

DOI: 10.1103/PhysRevLett.92.054801 PACS numbers: 41.75.Jv, 41.60.Cr

Using laser light to accelerate electrons to relativistic energies offers the potential for building more affordable high-energy accelerators. Laser-driven acceleration gradients >1 GV/m have been demonstrated [1], which means compact, table-top-sized accelerators for usage in industry, medicine, and academic research may be also possible. Advances in laser technology, such as the development of high-efficiency diode-pumped lasers [2], further enhances this effort.

Despite this exciting promise and the tremendous progress made in laser acceleration research, there has been little work to address the pragmatic problem of devising ways to make a useful laser-driven accelerator (laser linac). The >1-GV/m gradients have generally accelerated only a small fraction of the total available electrons and the energy spread of the accelerated electrons tends to be very large.

For efficient acceleration the electrons must be grouped together (i.e., microbunched) within a small fraction of the accelerating wave phase (e.g., $<\pi/2$). This is important in order for a large percentage of the electrons to be captured (''trapped'') within the laser field ponderomotive potential well (''bucket'') or laser-induced plasma wave, such as in plasma-based laser acceleration schemes [3]. During the acceleration process, the trapped electrons need to maintain a narrow energy spread (i.e., monoenergetic) so that in subsequent laser acceleration devices (''stages'') the electrons can continue to be efficiently trapped and accelerated. This staging process whereby a laser beam(s) repeatedly accelerates the electrons is fundamental for achieving high net acceleration.

It was the goal of our experiment, called staged electron laser acceleration (STELLA), to demonstrate all these features in a single system. To accomplish this we chose as our basic approach the concept of imparting a sinusoidal energy modulation on the electron beam (e beam), thereby leading to microbunching, and followed by monoenergetic acceleration with high-trapping efficiency. Thus, this experiment is fundamentally about validating a specific process for making a practical laser linac; it is not about further developing a particular laser acceleration mechanism.

Figure 1 illustrates the outcome of this microbunching process using a model simulation for the conditions of the STELLA experiment. Since the e-beam pulse length is much longer than the accelerating wavelength, the electrons initially enter uniformly distributed over all phases of the acceleration wave [Fig. 1(a)]. Exposing the electrons to an oscillating electromagnetic field causes sinusoidal energy modulation of the e-beam energy [Fig. 1(b)]. If these electrons are allowed either to drift or be sent through a bunch compressor device, then the fast electrons catch up with the slow ones [Fig. 1(c)] resulting in the creation of an $\approx$3-fs long [4] microbunch [Fig. 1(d)]. These microbunched electrons are sent through a second laser accelerator device at the proper phase with respect to the accelerating field in the second device to trap and accelerate the electrons while maintaining a narrow energy spread.

During a precursor experiment [4] of STELLA we demonstrated for the first time the microbunching and staging aspects illustrated in Fig. 1. This Letter describes the culmination of the STELLA experiment where high-trapping efficiency and monoenergetic laser acceleration are confirmed for the first time.

The basic STELLA concept can be applied to many different laser acceleration schemes. For experimental expediency and simplicity we chose to use inverse free

 © 2004 The American Physical Society

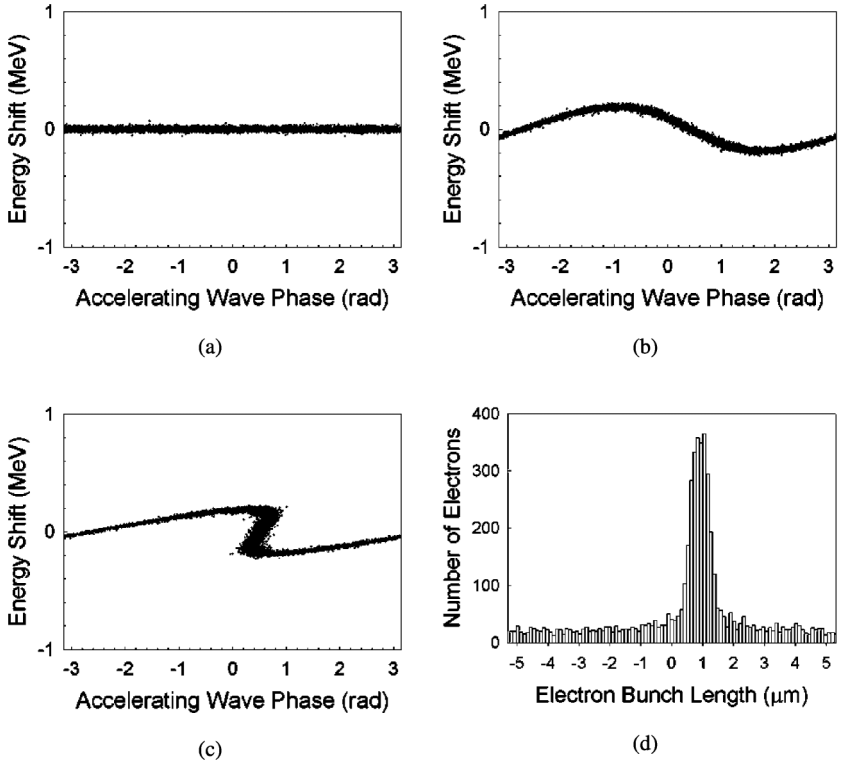

FIG. 1. Model simulation for STELLA showing the microbunching process. (a) *E*-beam energy shift from initial energy versus phase distribution relative to accelerating wave. (b) Energy-phase distribution after energy modulation by the first laser acceleration stage. (c) Energy-phase distribution after traveling through the bunch compressor (chicane). (d) Microbunch longitudinal density distribution of (c).

electron lasers [5] (IFEL) as our laser acceleration mechanism. An IFEL is a free electron laser operating in reverse. The laser beam copropagates with the *e* beam within the gap between a pair of parallel-facing magnet arrays called an undulator. Depending on the sign of the laser field seen by an electron, the electrons will be accelerated or decelerated.

STELLA is located at the Brookhaven National Laboratory Accelerator Test Facility (ATF). Figure 2 shows a schematic layout of the experiment. The ATF features a conventional microwave-driven linear accelerator [$E_0 = 45$ MeV, $\Delta E_0 = 0.03\%(1\sigma)$, $\varepsilon_n = 1.5$ mm-mrad$(\gamma\sigma\sigma')$, $q = 0.1$ nC, $\tau_e = 3$ ps(1σ)] and a >100-GW peak power CO_2 laser [$\lambda = 10.6$ μm, $\tau_l = 180$ ps (FWHM)]. The long wavelength of the CO_2 laser offers experimental advantages over the order-of-magnitude shorter wavelengths of solid-state lasers because the resynchronization requirements between the electrons and light wave are less stringent.

The *e* beam and the CO_2 laser beam are directed through the center of the first IFEL undulator (IFEL1), travel through a magnetic bunch compressor (chicane),

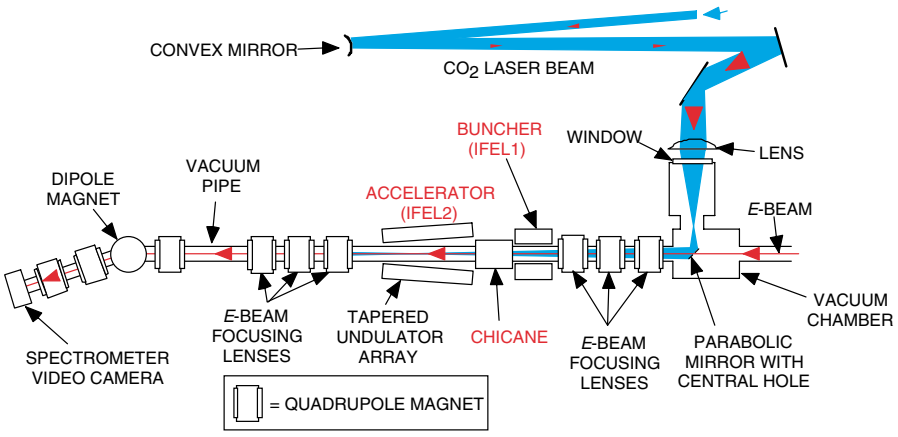

FIG. 2 (color online). Schematic layout for the STELLA experiment.

and finally are focused in the center of the second IFEL undulator (IFEL2). The purpose of IFEL1 is to impart the aforementioned sinusoidal energy modulation.

The chicane has both a fixed magnetic field (i.e., permanent magnets) and a variable magnetic field (i.e., electromagnets). The fixed field forces the electrons to travel through a "V-shaped" trajectory in which the faster electrons generated by IFEL1 traverse a shorter path than the slower ones, thereby causing the electrons to bunch at the entrance to IFEL2. This creates a train of microbunches (≈ 80 for a 3-ps e-beam pulse) separated by 10.6 μm with individual bunch lengths of ≈ 1 μm as predicted by our model [see Fig. 1(d)]. Control of the phase delay between the microbunches and the laser field in IFEL2 is achieved by adjusting the variable field of the chicane. This enables resynchronizing the microbunches with the accelerating portion of the laser field by slightly delaying when the electrons exit the chicane. Usage of the chicane also makes the entire system more compact with a total length of 1.2 m from IFEL1 to IFEL2.

IFEL2 used a tapered [6] undulator in which the gap separating the magnet arrays is smaller by 11% at the output end of the device (equivalent to 12% energy taper). Tapering is the key for achieving high-trapping efficiency and sufficient energy gain to separate the accelerated electrons from the background electrons. The laser field nominally accelerates the trapped electrons by the amount of energy taper of the undulator. Although the theoretical maximum amount of electrons in the microbunches produced by IFEL1 and the chicane is $\approx 50\%$, as explained later with high enough laser intensity driving IFEL2 it is possible to trap much more than 50% of the electrons [7].

Downstream of IFEL2 is an electron energy spectrometer with a resolution of $0.14\%(1\sigma)$, which is included in the model. Reference [8] has further details of the STELLA hardware specifications.

Two illustrative energy spectrum experimental results are presented along with model comparisons with the chicane phase delay set for maximum acceleration. The model [9] is a relatively simple, but comprehensive, PC-based 3D code. (Separate analysis and modeling results [10] show that space charge and coherent synchrotron radiation effects are not significant for the STELLA conditions.)

Figure 3(a) shows an example of high-trapping efficiency. Plotted on the abscissa is the energy shift from the initial e-beam energy. The ordinate represents the number of electrons of all the microbunches within a single 3-ps e-beam pulse, where the areas under the data and model curves have been normalized to each other. A large number of electrons have gained 7–9 MeV; in fact, an integration of the data curve indicates that $\approx 80\%$ of the electrons have been trapped and accelerated with an energy spread of $\approx 1.2\%(1\sigma)$.

The estimated laser intensity at the center of IFEL2 is 1.7–2.7 TW/cm^2. This agrees with the model simulation shown in Fig. 3(a), which used a laser intensity of 1.7 TW/cm^2. The predicted peak of the accelerated electrons agrees well with the data and has a similar amount of trapping efficiency, but has a narrower energy spread and two peaks near zero energy shift.

Figure 3(b) is the energy-phase plot for the prediction given in Fig. 3(a) and provides clues for the differences between the model and data. The double peaks near zero energy shift arise from untrapped electrons slipping over phase. The amount of slippage depends on a number of factors including the initial e-beam energy and the exact trajectory of the e beam relative to the undulator magnetic field. These affect the resonance condition and, therefore, how much phase slippage occurs while the electrons traverse through the undulator. The single peak of the data at zero energy shift seems to imply the actual resonance condition of the experiment was slightly different than in the model caused by, perhaps, misalignment through the undulator. This may also help explain the wider energy spread.

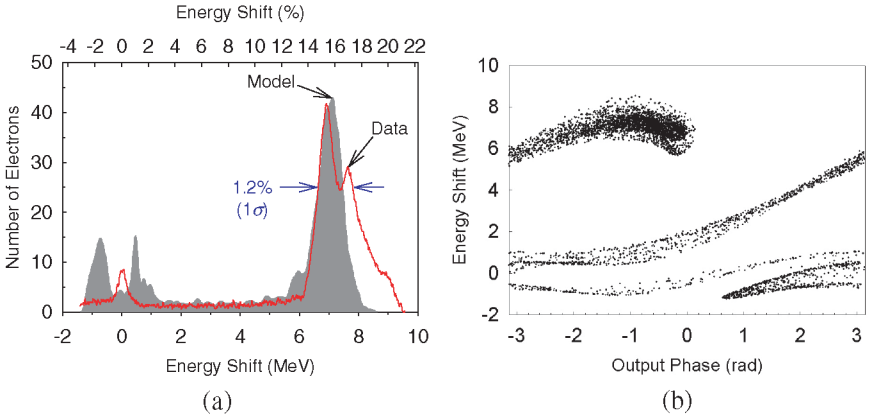

FIG. 3 (color online). (a) Example of electron energy spectrum for high-trapping efficiency case with the chicane phase delay set for maximum acceleration. The solid curve is data; the histogram (for 5000 electrons) is the model prediction with 1.7 TW/cm^2 driving IFEL2. (b) The energy-phase plot predicted by the model for simulation in (a).

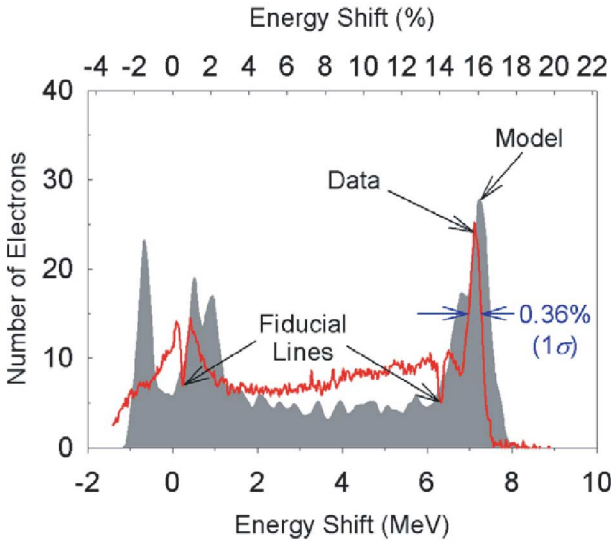

FIG. 4 (color online). Example of electron energy spectrum for narrow energy spread case with the chicane phase delay set for maximum acceleration. The solid curve is data; the histogram (for 5000 electrons) is the model prediction with 1.3 TW/cm^2 driving IFEL2. The two dips on the data curve designated as fiducial lines are caused by scribe lines on the spectrometer output screen.

Figure 3(b) also helps elucidate the high-trapping efficiency process. The microbunches initially start at the beginning of the undulator with zero energy shift. The deep laser potential well captures electrons neighboring in phase with the microbunch electrons and sweeps the ensemble up in energy as the electrons travel through the undulator resulting in the dense collection of electrons at 7–8 MeV seen in Fig. 3(b).

Figure 4 shows an example of a very narrow energy spread. The accelerated electrons still gained >7 MeV, but with an energy width of $\approx 0.36\%(1\sigma)$ and a smaller trapping efficiency of $\approx 14\%$. The lower trapping efficiency appears to be caused by a significant number of electrons lying between zero energy shift and 7 MeV.

A comparison with the model gives clues on the origin of these partially accelerated electrons. In Fig. 4 the laser intensity in the model was reduced to 1.3 TW/cm^2. This lower laser intensity primarily results in a narrower energy spread for the trapped electrons because the tapered undulator is being driven just above the threshold intensity for trapping [6]. However, the model also indicates that the partially accelerated electrons are due to a combination of an asymmetric e-beam focus within IFEL2 and an ~ 300 μm drift in spatial overlap between the e beam and the laser beam inside the tapered undulator. Essentially, the electrons start to interact with the laser beam at the beginning of the undulator in IFEL2, but later travel out of the laser beam towards the end of the undulator. Hence, they experience only partial energy gain. With symmetric e-beam focusing and good spatial overlap of the beams, the model predicts high-trapping efficiency with an energy spread of $<1\%(1\sigma)$.

During the experiment, the pulse-to-pulse energy fluctuation of the laser was $\pm 12\%$, which had a significant affect on the spectrum because the experiment primarily operated near threshold for trapping. As a first demonstration of high-trapping efficiency and monoenergetic acceleration, the experiment was not designed to explore the issue of stable injection and trapping.

For the 1-TW/cm^2 laser intensity and 45-MeV initial e-beam energy, analysis indicates the electrons enter near the bottom of the ponderomotive bucket, experience $\approx 1/2$ a synchrotron period movement inside the bucket while traveling through the undulator, and exit near the top of the bucket, thereby yielding additional acceleration beyond the amount of energy taper.

As a side benefit of this work, we have also shown that despite IFELs having certain scaling limitations, they are still useful devices for other applications. For example, they offer a convenient method for creating microbunches. Compact IFEL systems for producing ~ 1 GeV e beams may also be feasible [11].

In conclusion, we have successfully validated the basic approach of energy modulation, microbunching, trapping, and monoenergetic acceleration and, in doing so, demonstrated the crucial elements needed for a practical laser linac.

This work was supported by the U.S. Department of Energy, Grants No. DE-FG03-98ER41061, No. DE-AC02-98CH10886, and No. DE-FG03-92ER40695.

*Electronic address: wkimura@stioptronics.com

[1] See, for example, W. P. Leemans and E. Esarey, in *Advanced Accelerator Concepts*, edited by W. Lawson, C. Bellamy, and D. Brosius, AIP Conf. Proc. No. 472 (AIP, New York, 1999), p. 174.
[2] R. L. Byer, in *Advanced Accelerator Concepts*, edited by C. Joshi, AIP Conf. Proc. No. 193 (AIP, New York, 1989), p. 4.
[3] See, for example, A. Ting, F. Hubbard, and G. Shvets, in *Advanced Accelerator Concepts*, edited by C. E. Clayton and P. Muggli, AIP Conf. Proc. No. 647 (AIP, New York, 2002), p. 165.
[4] W. D. Kimura *et al.*, Phys. Rev. Lett. **86**, 4041 (2001).
[5] R. B. Palmer, J. Appl. Phys. **43**, 3014 (1972).
[6] N. M. Kroll, P. L. Morton, and M. Rosenbluth, IEEE J. Quantum Electron. **17**, 1436 (1981).
[7] D. C. Quimby, C. G. Parazzoli, and D. J. Pistoresi, Nucl. Instrum. Methods Phys. Res., Sect. A **318**, 628 (1992).
[8] W. D. Kimura *et al.*, in *Advanced Accelerator Concepts* (Ref. [3]), p. 269.
[9] W. D. Kimura *et al.*, Phys. Rev. ST Accel. Beams **4**, 101301 (2001).
[10] F. Zhou, D. B. Cline, and W. D. Kimura, Phys. Rev. ST Accel. Beams **6**, 054201 (2003).
[11] E. D. Courant, C. Pellegrini, and W. Zakowicz, Phys. Rev. A **32**, 2813 (1985).